NASA TECHNICAL NOTE

NASA TN D-3065

NASA TN D-3065

DAMPING CHARACTERISTICS OF BUILT-UP CANTILEVER BEAMS IN A VACUUM ENVIRONMENT

by Robert R. McWithey and Robert J. Hayduk

Langley Research Center
Langley Station, Hampton, Va.

NATIONAL AERONAUTICS AND SPACE ADMINISTRATION • WASHINGTON, D. C. • NOVEMBER 1965

NASA TN D-3065

DAMPING CHARACTERISTICS OF BUILT-UP CANTILEVER BEAMS IN A VACUUM ENVIRONMENT

By Robert R. McWithey and Robert J. Hayduk

Langley Research Center
Langley Station, Hampton, Va.

NATIONAL AERONAUTICS AND SPACE ADMINISTRATION

For sale by the Clearinghouse for Federal Scientific and Technical Information
Springfield, Virginia 22151 – Price $2.00

DAMPING CHARACTERISTICS OF BUILT-UP CANTILEVER BEAMS IN A VACUUM ENVIRONMENT

By Robert R. McWithey and Robert J. Hayduk
Langley Research Center

SUMMARY

Damping measurements have been made on solid and built-up cantilever beams in a vacuum environment to determine the effects on structural damping. The changes in damping characteristics are noted for various values of clamping pressure between beam laminates for the case of the built-up beam. Results indicate no significant changes in structural damping characteristics as a result of exposure to pressures as low as 1×10^{-9} torr (0.13 $\mu N/m^2$).

INTRODUCTION

The amount of structural damping present in a built-up structure may be significantly altered if the environmental conditions to which the structure is subjected allow the phenomenon of cold welding to occur. In the case of built-up structures, the sliding motion present between contact surfaces may expose "clean" surfaces which have been shown to weld together at room temperature in a vacuum environment. (See refs. 1 to 4.) This bonding of the contact surfaces would retard motion between them which, in turn, would result in a change in the amount of structural damping present in the vibrating structure.

Reported herein are the results of a preliminary investigation to determine the amount of structural damping produced by a simple built-up structure and the effect of vacuum on its damping characteristics. The units used for the physical quantities defined in this paper are given both in the U.S. Customary Units and in the International System of Units (SI). Factors relating the two systems are given in reference 5 and those used in the present investigation are presented in the appendix.

TEST APPARATUS

Vacuum System

The vacuum system used in this investigation (fig. 1) consists of a horizontal cylindrical chamber, one oil-diffusion pump, 10 inches (25.4 cm) in diameter, with water-cooled baffle, an optically dense liquid-nitrogen baffle, and

a 40 ft^3/min (19 dm^3/s) rotary mechanical pump. The system is designed for continuous operation and is capable of reaching pressures below 1×10^{-9} torr ($0.13\ \mu N/m^2$). A characteristic pressure history for the system with a clean dry chamber is shown in figure 2. The stationary pressure with a clean dry chamber and with only the mechanical pump operating is approximately 5×10^{-3} torr ($0.67\ N/m^2$).

The chamber is a vessel of type 304 stainless steel with an inside diameter of 30 inches (76 cm) and a length of 48 inches (122 cm), excluding the dished heads. One of the dished heads is removable to allow access to the interior of the chamber. Mounted in the chamber ports are a bellows-sealed push-pull feedthrough with a maximum travel of 2 inches (5.1 cm) and a designed axial-force load capacity of 75 pounds (334 N), one electrical feedthrough containing 54 carry-through pins for internal power and instrumentation, two sight glasses, and one blank disk. The ports have matching flanges so that feedthroughs and sight glasses may be interchanged. All flanges on the high-vacuum side of the diffusion pump may be sealed with double "O" rings to allow circulation of liquid coolant or with copper "O" rings. Flanges on the high-vacuum side of the diffusion pump which are sealed with double "O" rings incorporate fluoroelastomer "O" rings in the inner ring and silicone "O" rings in the outer ring. In the test program reported herein, copper "O" rings were used on the electrical feedthrough flange, the blank flange, and the push-pull feedthrough flange. The exterior of the chamber is traced with stainless-steel tubing to allow circulation of liquid coolant. Chilled water for the chamber is provided by the refrigeration system shown in figure 3.

Chamber bakeout is achieved by means of an oven, supported on tracks, which is rolled over the chamber during the bakeout period. (See fig. 3.) A platform attached to the chamber support frame directly below the chamber serves as the oven floor. Bakeout temperatures are thermostatically controlled and normally are limited to a maximum temperature of 325° F (436° K).

Pressure readings are obtained by means of two modified, Bayard-Alpert type, ionization gages located on top of the chamber near the access door, three thermocouple gages located along the pumping line, and a dial gage for measuring pressures within the chamber from atmospheric pressure to 1.0 torr ($133\ N/m^2$). The approximate location of these gages is shown in figure 1. Gage controls are mounted in an instrumentation cabinet as shown in figure 4. Other controls in this cabinet include switches for the diffusion pump, the mechanical pump, and the bakeout oven, and a six-position thermocouple-gage selector.

Test Specimens

The test specimens were three cantilever beams machined from normalized SAE 4130 steel to a root-mean-square surface finish of 32 microinches (0.81 μm). The beams had a cantilever-beam length of 20.0 inches (50.8 cm), a nominal depth of 0.25 inch (0.64 cm), and a width of 1 inch (2.54 cm). Details of the beam dimensions are shown in figure 5; the three beams, designated a, b, and c, were solid, rivet fastened, and screw fastened, respectively. The riveted beam

was fastened with two rows of spherical-head rivets, $\frac{1}{8}$ inch (0.32 cm) in diameter, each row consisting of 33 rivets spaced longitudinally 0.60 inch (1.52 cm) apart, and with their centers 0.27 inch (0.69 cm) from the edge of the beam. The rivets were driven tight while cold and were assumed to fill the holes. Beam c was fastened with two rows of No. 6-40 socket-head cap screws located identically as the spherical-head rivets were in beam b. Matching patterns of tapped holes in the bottom laminate and clearance holes in the top laminate gave a radial clearance of 0.003 inch (76 μm) between the threads of the screws and the top laminate. This clearance is sufficient to eliminate the possibility of contact between the screw threads and the top laminate.

Specimen Support and Deflecting Mechanism

The beams were mounted in hardened-steel clamping blocks on a stainless-steel pedestal which was bolted to a mounting plate attached to the chamber wall. This supporting structure is shown in figure 6. Details of the clamping blocks are shown in figure 7. It may be seen that the clamping blocks are designed to allow high clamping pressure to be applied on the test specimens by tightening the four bolts which extend through the clamping blocks and attach to the pedestal. The slots in the bottom clamping block make a push fit with the test specimen and allow accurate positioning of the test specimen when it is inserted in the block.

Specimen deflection within the vacuum system is attained by means of a hook mechanism attached to the push-pull feedthrough located in the bottom chamber port. (See fig. 6.) This mechanism is designed to engage and deflect the beam downward a preset distance and automatically release the beam. The hook may be positioned for reengagement by returning the push-pull feedthrough to the up position. Figure 8 shows the hook-mechanism positions during engagement and after release of the beam.

TEST INSTRUMENTATION

Vertical deflections at the tip of the cantilever beam were recorded during the tests by connecting the output of a commercially available optical-electronic transducer to a direct-recording oscillograph. The transducer components include a cathode-ray tube, an optical system, a phototube, and supporting electronics. A schematic of the system is shown in figure 9. When in operation, a small light spot, produced by the cathode-ray tube, is focused on the edge of the mirror attached to the tip of the test beam. If the spot of light remained stationary, any vertical motion of the mirror would result in a large change in the amount of light reflected back to the phototube. The output of the phototube, however, is connected to the deflection plates of the cathode-ray tube and drives the light spot, focused on the test-beam mirror, in the direction of motion of the test beam. Therefore, the closed system formed by the cathode-ray tube, optical system, and phototube keeps this light spot fixed to the reflective discontinuity on the surface of the test specimen (i.e., the edge of the mirror) and hence, as the specimen is deflected, the light spot

remains fixed to this location. The output from the phototube, which produces an output proportional to tip displacement of the cantilever beam, thus serves as a measure of the specimen deflection and is used to control the input to the recording oscillograph. Only displacements in a direction normal to the optical axis of the transducer may be measured and the system must be operated in total darkness. The instrumentation setup is shown in figure 10.

TEST PROCEDURE

General

Tests were conducted on all beams at atmospheric pressure and at reduced pressures as low as 1×10^{-9} torr (0.13 $\mu N/m^2$). The apparatus and instrumentation used permitted only one beam to be tested at a time. Temperature measurements obtained from a beam similar to those tested and positioned similarly within the vacuum chamber indicated that the test-beam temperature would not vary from room temperature during the tests. Therefore, no attempt was made to control or measure the test-beam temperature.

After the test beam had been cleaned by means of a caustic bath and acetone, it was dried with a hot-air blower and mounted on the pedestal inside the vacuum chamber. The light spot of the optical-electronic transducer was then focused on the tip of the beam, and a test was made at atmospheric pressure. All tests consisted of deflecting and releasing the beam by means of the hook mechanism and recording the resultant tip deflection of the lightly damped vibrating beam with the direct-recording oscillograph. The initial tip deflection in all tests was 7/16 inch (1.1 cm). Data at reduced pressures were obtained first by evacuating the chamber with the mechanical pump and conducting several tests between atmospheric pressure and the blank-off pressure of the system with only this pump in operation. The diffusion pump was then turned on and the liquid-nitrogen baffle was immediately filled with liquid nitrogen in order to minimize the back stream of oil vapor into the chamber. Tests were made at each decade of pressure. The beams were exposed to the lowest decade of pressure (usually the range from 1×10^{-9} to 10×10^{-9} torr (0.13 to 1.31 $\mu N/m^2$)) for a period from 2 days to 2 weeks in order to determine the effect of prolonged exposure on the damping characteristics of the beam.

In tests conducted on the screw-fastened beam, screw torque was adjusted by using a torque wrench capable of applying torque from 0 to 30 inch-pounds (0 to 3.39 m-N) for the settings of 5, 10, 15, and 20 inch-pounds (0.56, 1.13, 1.69, and 2.26 m-N, respectively), and a torque wrench capable of applying from 0 to 6 inch-ounces (0 to 0.042 m-N) of torque for the smaller torque settings.

Method of Damping Measurement

The damping properties of lightly damped vibratory motion may be described by various methods involving the ratio of energy loss per cycle to total strain energy of the vibrating system. A commonly used unit employed throughout this

paper is the logarithmic decrement. By definition (refs. 6 and 7), the logarithmic decrement over one period of vibration is given by:

$$\delta_m = \frac{\Delta E_m}{2E_m} = \ln \frac{y_{m-1}}{y_m} \tag{1}$$

where ΔE_m is the energy dissipated during the mth cycle, E_m is the strain energy present at the beginning of the mth cycle (time of maximum deflection), y_{m-1} is the amplitude at the beginning of the cycle, and y_m is the amplitude at the end of the cycle. If an arithmetic mean for δ_m over n consecutive cycles is calculated, equation (1) gives

$$\delta = \frac{1}{n} \ln \frac{y_0}{y_n} \tag{2}$$

where δ is the arithmetic mean value of the n values of logarithmic decrement, y_0 is the maximum amplitude in the first cycle being considered, and y_n is the amplitude at the end of the last cycle being considered. In reducing data obtained from the tests reported herein, the equation similar to equation (2) which was used is

$$\delta = \frac{1}{n} \ln \frac{y_k}{y_{k+n}} \tag{3}$$

where δ is the logarithmic decrement, y_k is the peak-to-peak oscillograph-trace deflection after k cycles (fig. 11), y_{k+n} is the peak-to-peak oscillograph-trace deflection after $k+n$ cycles, and n is the number of cycles between k and $k+n$. The use of this equation results in an arithmetic mean value of the logarithmic decrement between y_k and y_{k+n}. Corresponding values of tip deflection were obtained by converting the values of y_k, recorded during the vibration decay, to the actual tip amplitude in inches. These data were used to prepare figures 12, 13, and 14.

TEST RESULTS AND DISCUSSION

In order to determine the effectiveness of the support system in making the clamped-end condition of the beam a true cantilever, theoretical first-bending-mode frequencies for a cantilever beam were compared with those obtained experimentally. This comparison was made for each beam and the results are shown in table I. The theoretically determined frequencies are based upon elementary beam theory and include the effect of the concentrated mass of the mirrors at the tip of the beam. The mass of the rivet heads and screw heads was assumed to be uniformly distributed along the length of the beam. The experimental frequency for the screw-fastened beam was obtained for a screw torque of 20 inch-pounds (2.26 m-N). The excellent agreement between the experimental frequency

values and the theoretically obtained frequencies indicates that the boundary conditions for the test beam very closely approximate the boundary conditions for a true cantilever beam.

Inasmuch as the fixed-end conditions were the same for tests on all three beams, the magnitude of damping for the solid beam was used as an indication of the damping contributions of the support system, beam material, and air drag. Logarithmic decrements δ are plotted against tip amplitude for the solid beam at two pressures in figure 12. The curves show that the solid beam is lightly damped and that, within the range of vacuum attained, the vacuum environment has no significant effect on the damping characteristics of the beam. Also, for the larger amplitudes, the amount of damping present is always slightly greater at atmospheric pressure than that at the reduced pressure. This increase in damping is probably caused by the damping effects of the surrounding air. Results of reference 8 indicate that, for large-amplitude vibrations, the damping caused by air pressure drag and viscous-air drag may become a significant portion of the damping present at atmospheric pressure and that these contributions to damping become negligible below 10 torr (13 hN/m^2).

Similar results are shown in figure 13 for the rivet-fastened beam. The close agreement between the values of logarithmic decrement for both the solid beam and riveted beam was expected inasmuch as the rivets in the rivet-fastened beam were driven tight, completely filling the holes in the beam. This method of fabrication precludes relative motion between the laminates, virtually eliminating slip damping.

The most interesting data resulted from the tests on the screw-fastened beam. These tests were conducted both at various ambient pressures and at various values of screw torque. Curves of logarithmic decrement plotted against tip amplitude obtained from the test data for the various test conditions are shown in figure 14. It should be noted that the curves of figure 14 represent the total damping present in the beam. The contribution due to slip damping is the difference between values of logarithmic decrement for the solid beam (fig. 12) and values of logarithmic decrement given in figure 14 for corresponding amplitudes. Thus, figure 14(a) indicates that slip damping is a significant portion of the total damping present for a screw torque of 0.375 inch-pound (0.0423 m-N), whereas the damping curves for the remaining values of screw torque shown in figures 14(b) to (e) indicate that slip damping is not a significant portion of the total damping. The characteristics of the curves in figure 14(a) differ from the comparable curves in figures 12, 13, and 14(b) to (e) in two other respects. First, the slopes of the curves in figure 14(a) decrease with increasing amplitude, whereas the comparable curves indicate an increase in slope with increasing amplitude. Second, the damping curve obtained for the low ambient pressure in figure 14(a) indicates a substantially higher logarithmic decrement at the lower amplitudes. Although errors in the indicated values of logarithmic decrement in figure 14(a) may vary from ± 4 percent at the high amplitudes to ± 50 percent at the low amplitudes, the characteristics of the curves were confirmed by repeated tests both at atmospheric pressure and at reduced pressure for this value of screw torque.

A clear explanation for the variation in slope of the slip-damping curves would involve an analysis in which an inertia loading along the length of the

beam would be used in place of a concentrated force at the tip, as was done in reference 9. The inertia loading, of course, makes the shear at the interface a function of position along the length of the beam and greatly increases the complexity of the analysis. However, the gross results in reference 9 for the preslip condition, which are comparable to the results in figure 14(a), indicate that in the range of small amplitudes a large increase in slip damping occurs with increasing amplitude. Also, the slopes of the comparable curves in reference 9 range from some relatively large positive value at the lower amplitudes to zero at amplitudes corresponding to a logarithmic decrement value of approximately 0.75.

An explanation for the change in slip damping due to variation in ambient pressure, as shown in figure 14(a), was found in the results of additional tests conducted at atmospheric pressure at various screw torques. The results of these tests are shown in figure 15. It may be seen from the figure that only low values of screw torque produce significant effects on damping. The test point shown for zero screw torque is the approximate amount of damping present for both the solid beam and the built-up beam with all screws removed. Therefore, the damping-torque curve passes through some maximum value between zero and 1 inch-pound (0.113 m-N) of torque. This result is in agreement with the results found in reference 9, which show that at zero clamping pressure the slip damping is zero, and at high clamping pressures the slip damping again is zero; at some intermediate clamping pressure the slip damping reaches a maximum value. From figure 15, it can be seen that maximum slip damping would occur for a screw torque slightly greater than 0.375 inch-pound (0.042 m-N).

Thus, the following explanation for the observed increase in damping at the low ambient pressure may be formulated. The force producing the slip damping is the frictional force present at the interface of the beam laminates and has a value equal to the product of the coefficient of friction μ and the normal force, which is comparable to screw torque. Consequently, curves describing damping as a function of normal force, or screw torque, for constant μ would have characteristics identical to those describing damping as a function of μ for constant screw torque. Therefore, curves of slip damping plotted against μ for values of screw torque less than that producing maximum slip damping (such as the value of 0.375 inch-pound (0.042 m-N)) would have a positive slope until the product of μ and the screw torque exceeded that which produces maximum slip damping. Consequently, the increase in damping as noted in figure 14(a) at the low ambient pressure would occur as a result of an increase in μ. The result shown in figure 14(a), therefore, should be expected if some cold welding is occurring at the interface of the beam laminates.

Similar arguments may be used to explain either decreases or no changes in slip damping with changes in ambient pressure using, respectively, either the negative slope portion or the zero slope portion of the curve shown in figure 15.

The beam frequency was nearly constant over the range of torques used, with the exception of the condition for zero torque. (See fig. 16.) The nearly constant frequency results indicate that even a relatively small clamping pressure causes approximately integral beam vibration; that is, the effective moment of inertia of the beam cross section remains nearly constant. The frequency value

for the beam at zero screw torque is what would be expected for the two laminates acting independently.

CONCLUDING REMARKS

An investigation to determine the effect of a vacuum environment on slip damping was conducted using three cantilever beams as test specimens. One of the test specimens, a solid beam, was used to measure the amount of damping present in the support apparatus and beam material in the absence of slip damping. The other test specimens were built-up beams, one of which had rivet-fastened laminates, and the other screw-fastened laminates.

Slip damping was found to predominate only in the screw-fastened beam at low values of screw torque, and test results indicated a slight increase in damping due to the vacuum environment. An explanation for this phenomenon is given based upon work by Goodman and Klumpp (Journal of Applied Mechanics, September 1956) and the occurrence of cold welding.

In tests in which slip damping is insignificant, no changes in damping characteristics were observed between the atmospheric-ambient-pressure tests and low-ambient-pressure tests other than a slightly greater damping value at large amplitudes at atmospheric pressure due to air damping. The magnitude of damping was nearly constant for the various test conditions and, except for the condition of zero torque, the beam frequency was nearly constant.

Langley Research Center,
National Aeronautics and Space Administration,
Langley Station, Hampton, Va., June 23, 1965.

APPENDIX

CONVERSION OF U.S. CUSTOMARY UNITS TO SI UNITS

The International System of Units (SI) was adopted by the Eleventh General Conference on Weights and Measures, Paris, October 1960, in Resolution No. 12 (ref. 5). Conversion factors for the units used herein are given in the following table:

Physical quantity	U.S. Customary Unit	Conversion factor (*)	SI unit
Length	inch	0.0254	meters (m)
Pressure	torr	133.322	newtons per square meter (N/m^2)
Temperature	(^oF + 459.67)	5/9	degrees Kelvin (^oK)
Torque	inch-pounds	0.112985	meter-newton (m-N)
Torque	inch-ounces	0.000706	meter-newton (m-N)
Force	pounds	4.448	newtons (N)
Miscellaneous	ft^3/min	0.000472	cubic meters per second (m^3/s)

*Multiply value given in U.S. Customary Unit by conversion factor to obtain equivalent value in SI unit.

Prefixes to indicate multiple of units are as follows:

Prefix	Multiple
micro (μ)	10^{-6}
milli (m)	10^{-3}
centi (c)	10^{-2}
deci (d)	10^{-1}
hecto (h)	10^{2}

REFERENCES

1. Freitag, E. H.: The Friction of Solids. Contemp. Phys., vol. 2, no. 3, Feb. 1961, pp. 198-216.

2. Ham, John L.: Investigation of Adhesion and Cohesion of Metals in Ultrahigh Vacuum - March 1, 1963 to November 1, 1963. NRC Proj. No. 81-1-0101 (Contract No. NASw-734), Natl. Res. Corp. (Cambridge, Mass.), Nov. 27, 1963.

3. Ham, John L.: Investigation of Adhesion and Cohesion of Metals in Ultrahigh Vacuum - June 15, 1961 to July 31, 1962. NRC Proj. No. 42-1-0121 (Contract No. NASr-48), Natl. Res. Corp. (Cambridge, Mass.), Sept. 7, 1962.

4. Bowden, F. P.; and Rowe, G. W.: The Adhesion of Clean Metals. Proc. Roy. Soc. (London), ser. A, vol. 233, no. 1195, Jan. 10, 1956, pp. 429-442.

5. Mechtly, E. A.: The International System of Units - Physical Constants and Conversion Factors. NASA SP-7012, 1964.

6. Thomson, William Tyrrell: Mechanical Vibrations. Second ed., Prentice-Hall, Inc., c.1953.

7. Plunkett, R.: Measurement of Damping. Structural Damping, Jerome E. Ruzicka, ed., Am. Soc. Mech. Engrs., c.1959, pp. 117-131.

8. Baker, W. E.; and Allen, F. J.: The Damping of Transverse Vibrations of Thin Beams in Air. Rept. No. 1033, Ballistic Res. Labs., Aberdeen Proving Ground, Oct. 1957.

9. Goodman, L. E.; and Klumpp, J. H.: Analysis of Slip Damping With Reference to Turbine-Blade Vibration. J. Appl. Mech., vol. 23, no. 3, Sept. 1956, pp. 421-429.

TABLE I.- THEORETICAL AND EXPERIMENTAL FIRST-BENDING-MODE FREQUENCIES

Beam specimen	Frequency, cps	
	Theoretical	Experimental
Solid	20.189	20.061
Rivet fastened	19.740	19.658
Screw fastened	19.691	[a]19.057

[a]Obtained for a torque of 20 inch-pounds (2.26 m-N).

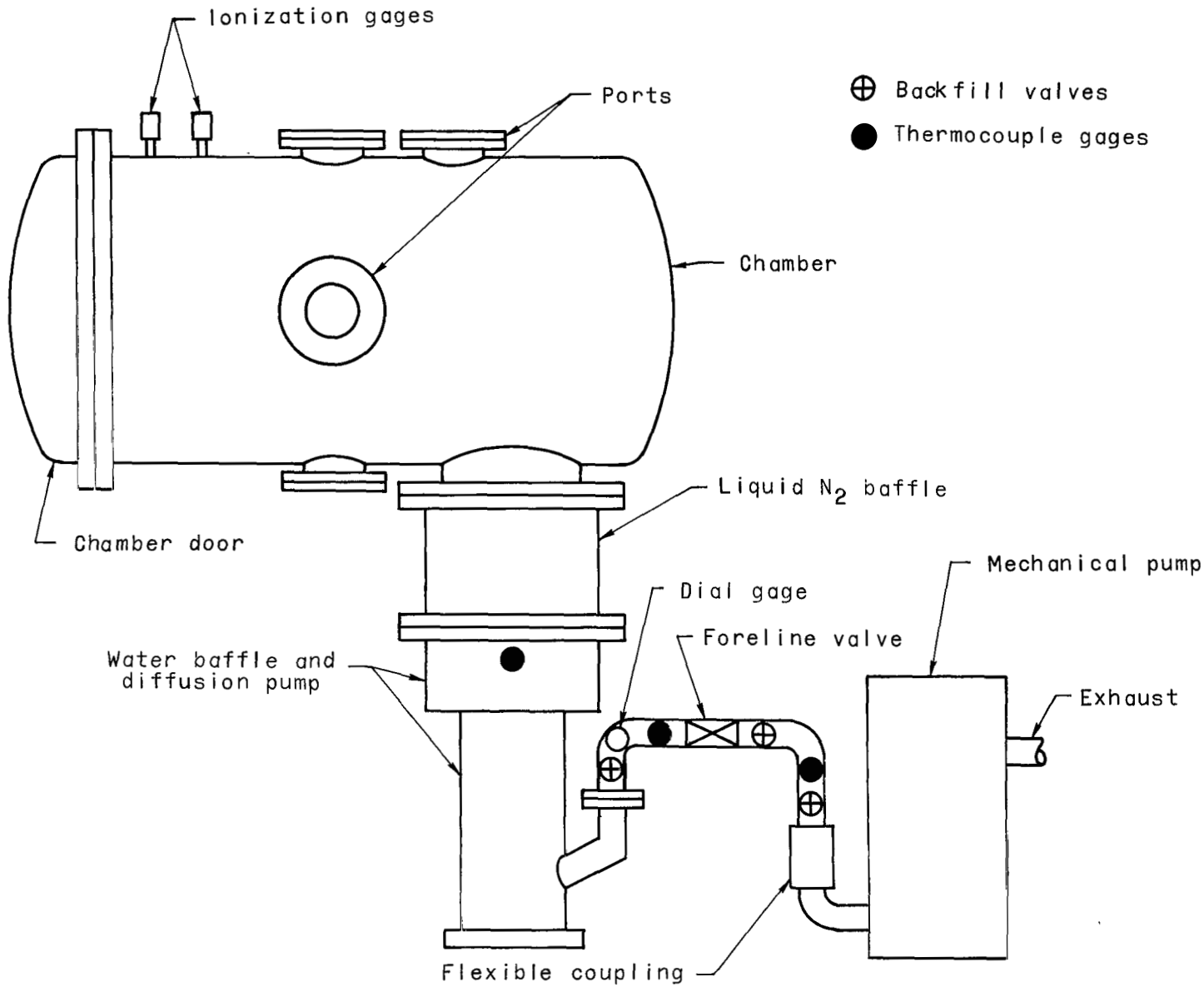

Figure 1.- Schematic diagram of vacuum system.

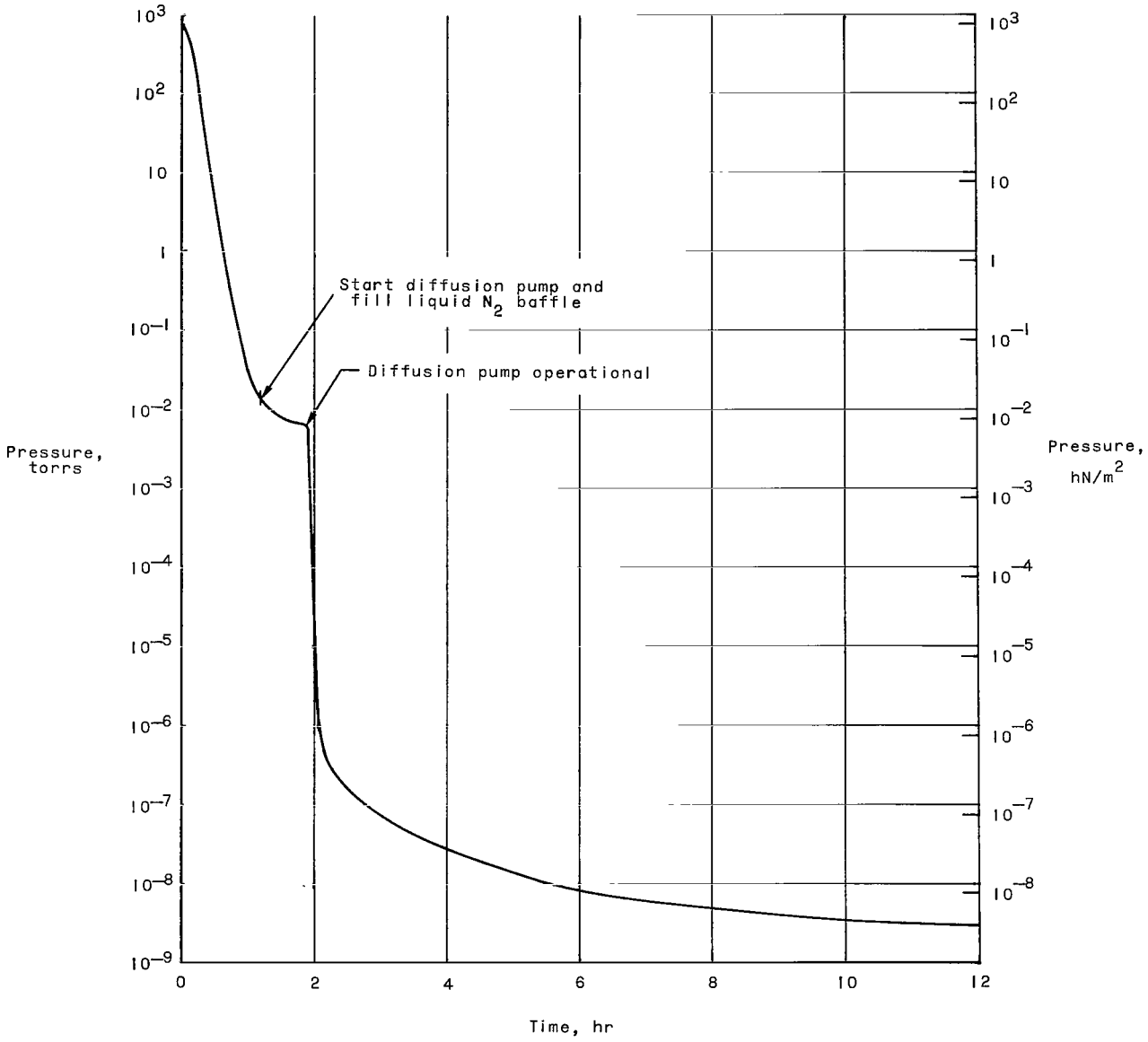

Figure 2.- Characteristic pressure history for vacuum system.

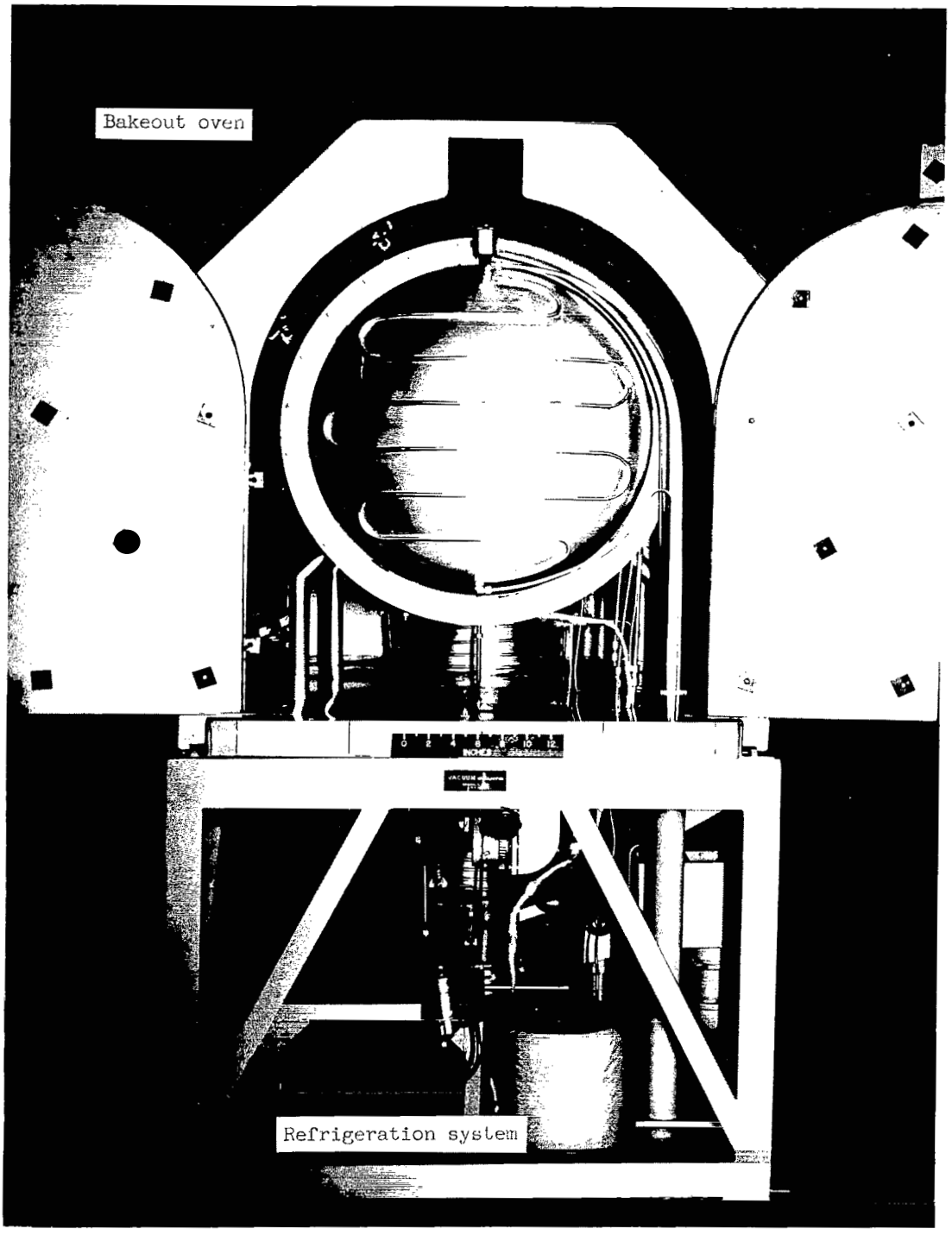

Figure 3.- Refrigeration system and bakeout oven for vacuum system. L-63-1999.1

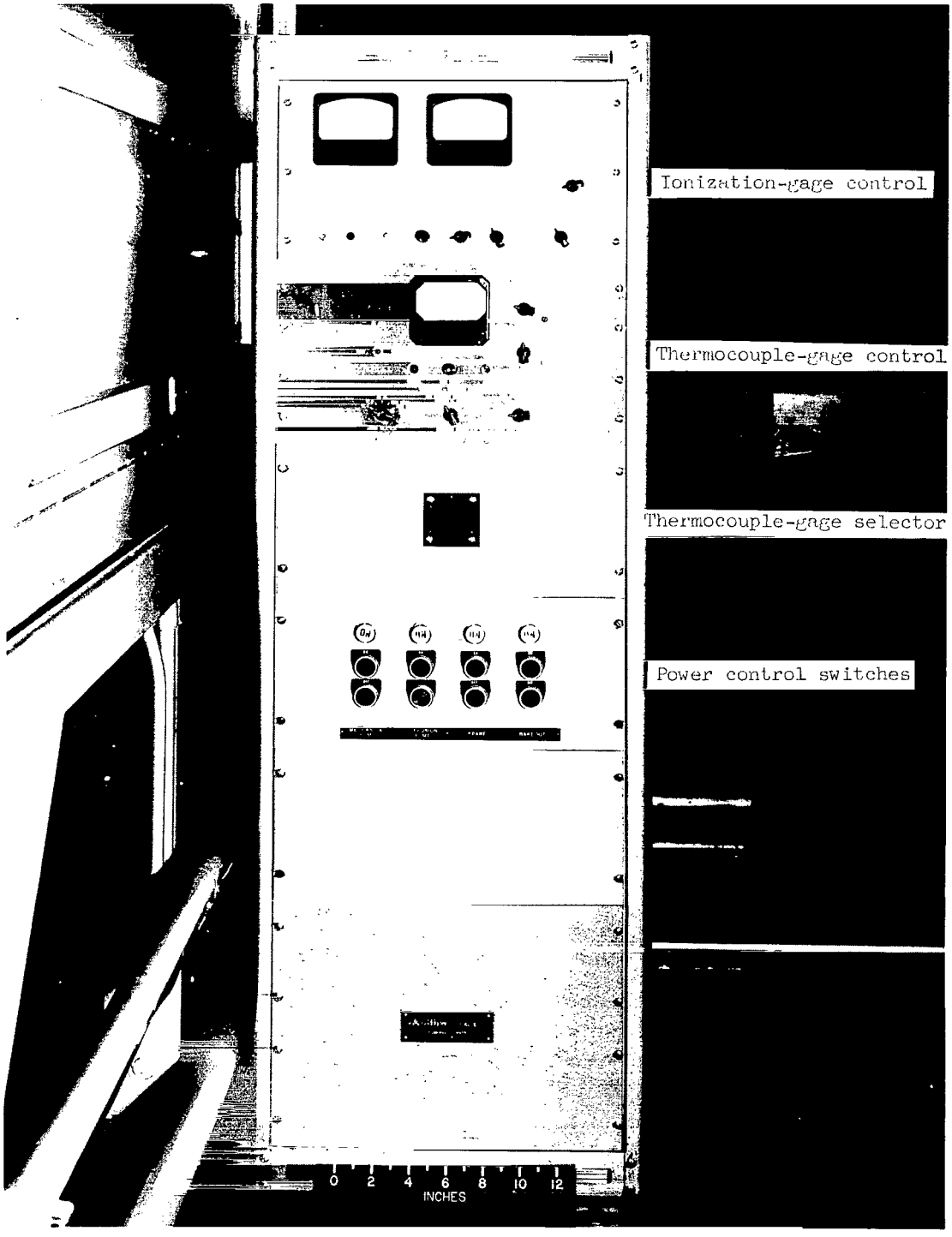

Figure 4.- Instrumentation cabinet for vacuum system. L-63-1993.1

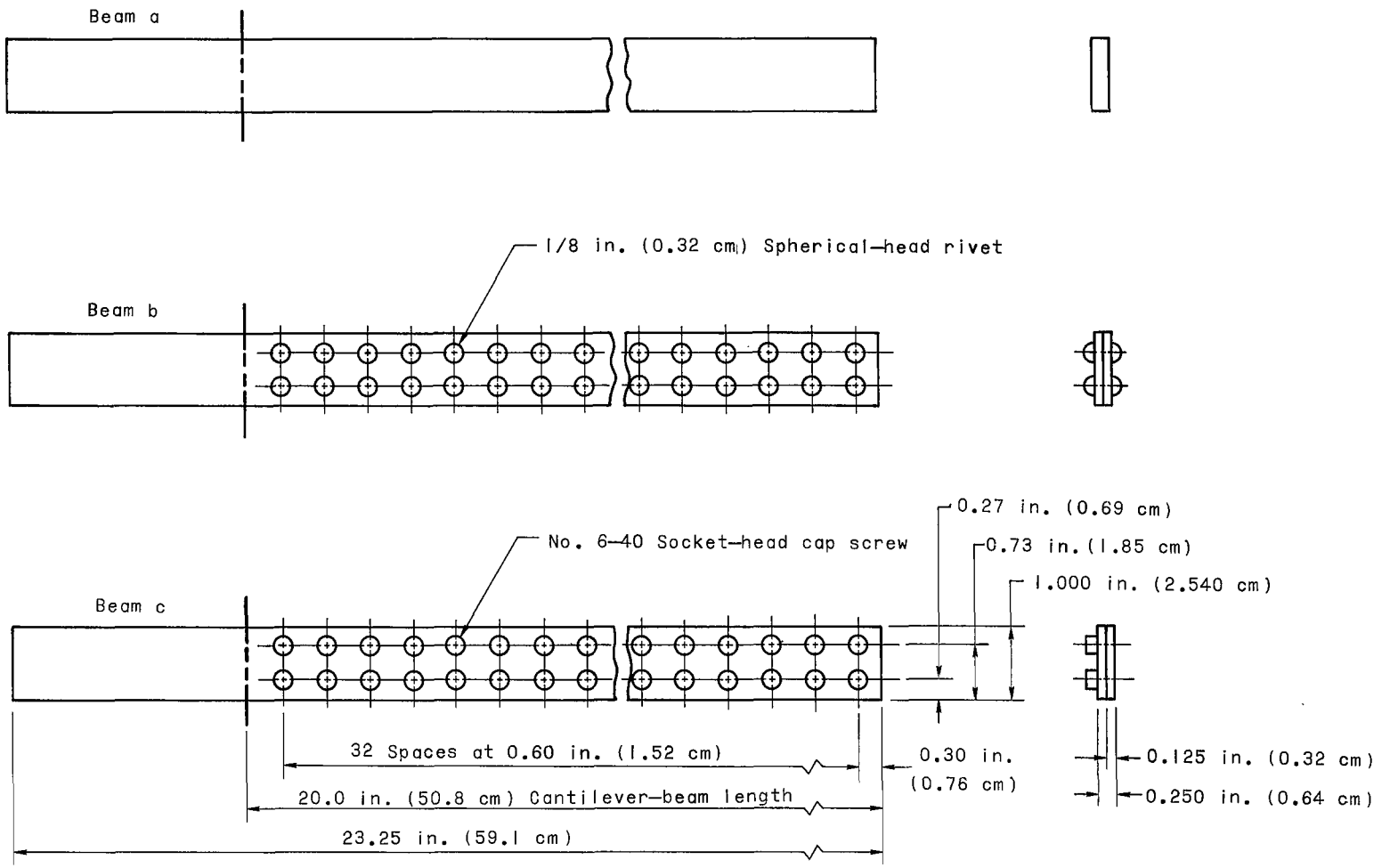

Figure 5.- Details of test specimens.

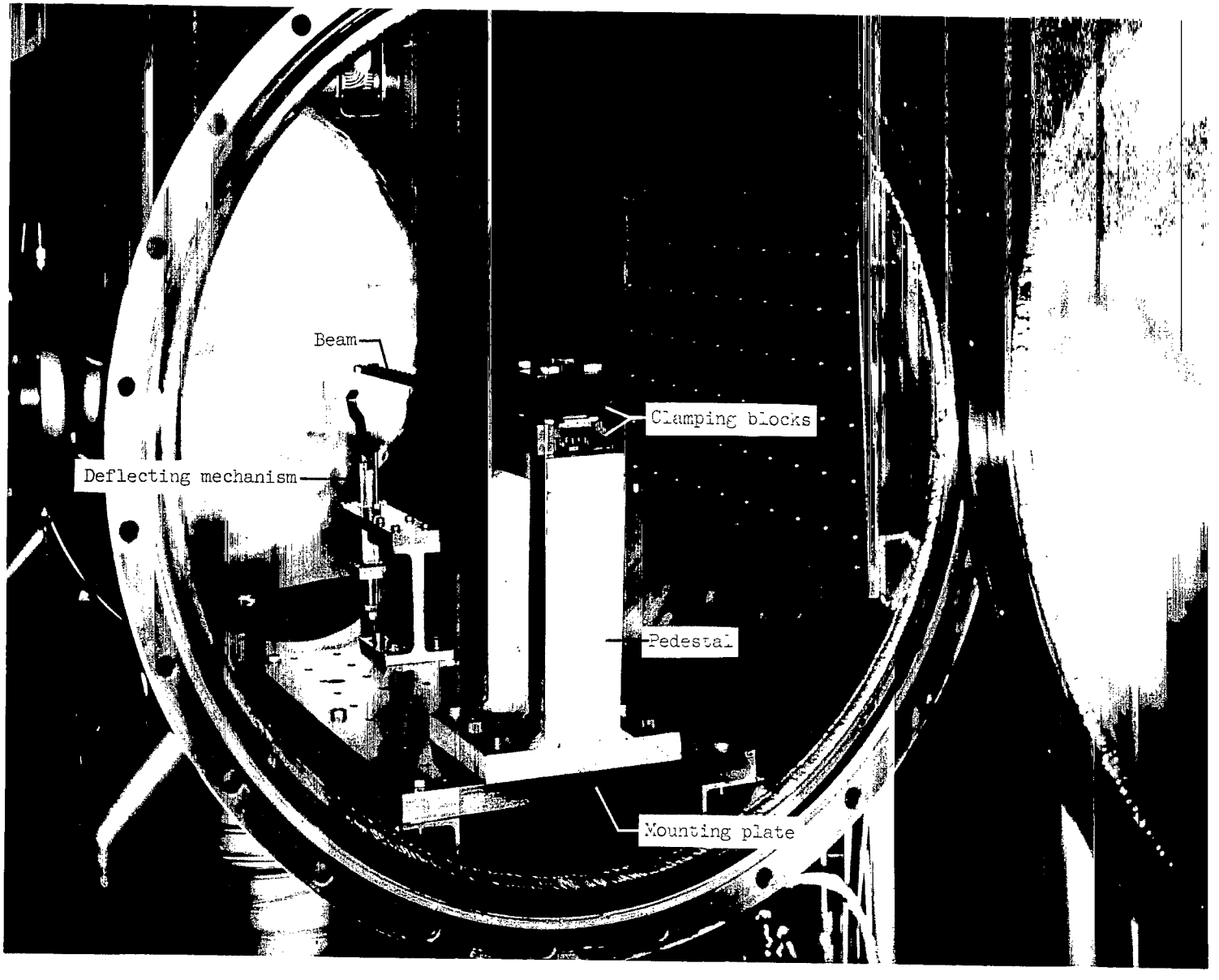

Figure 6.- Supporting structure for test specimens.

L-63-1991.1

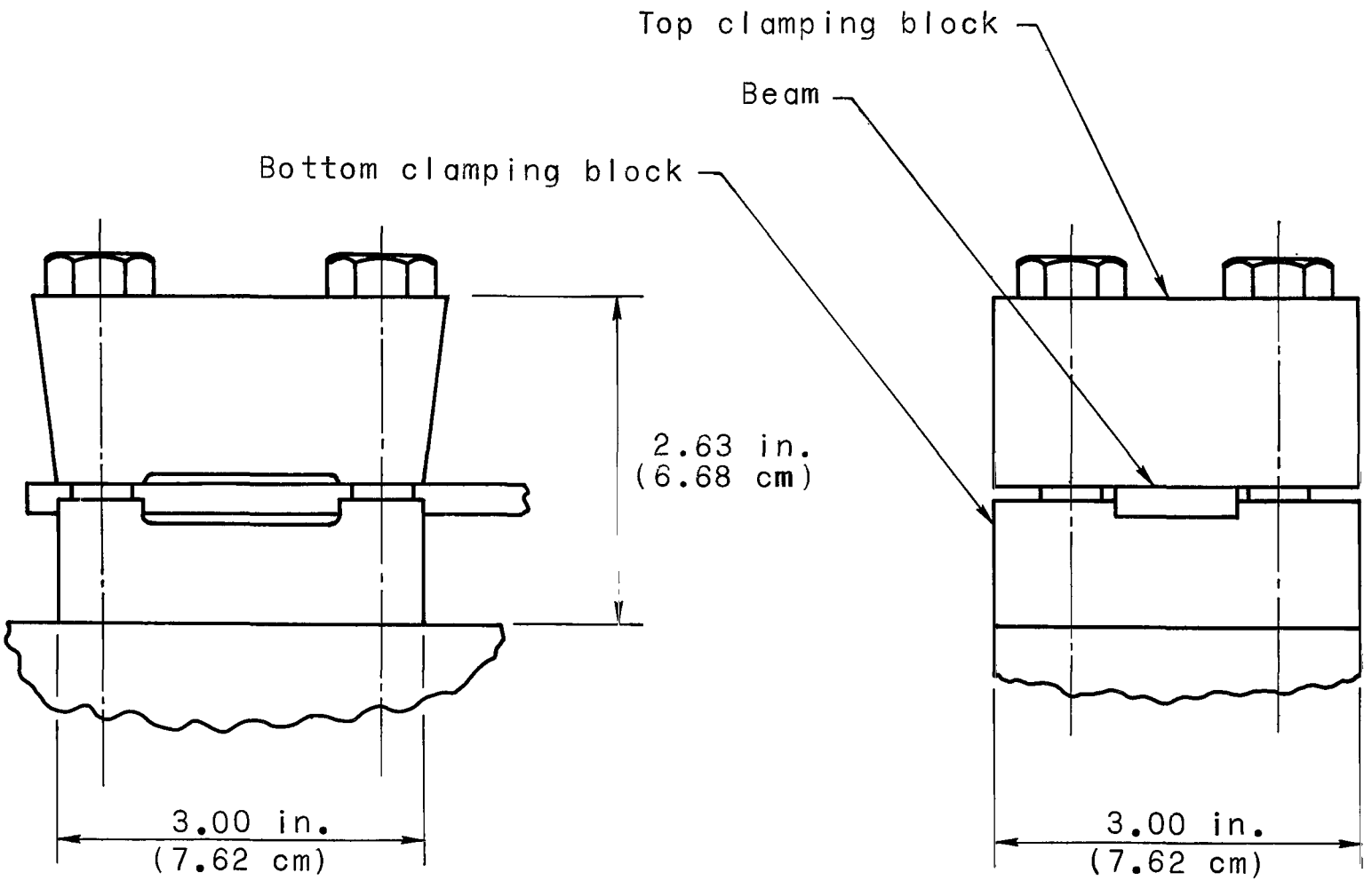

Figure 7.- Details of test-specimen clamping blocks.

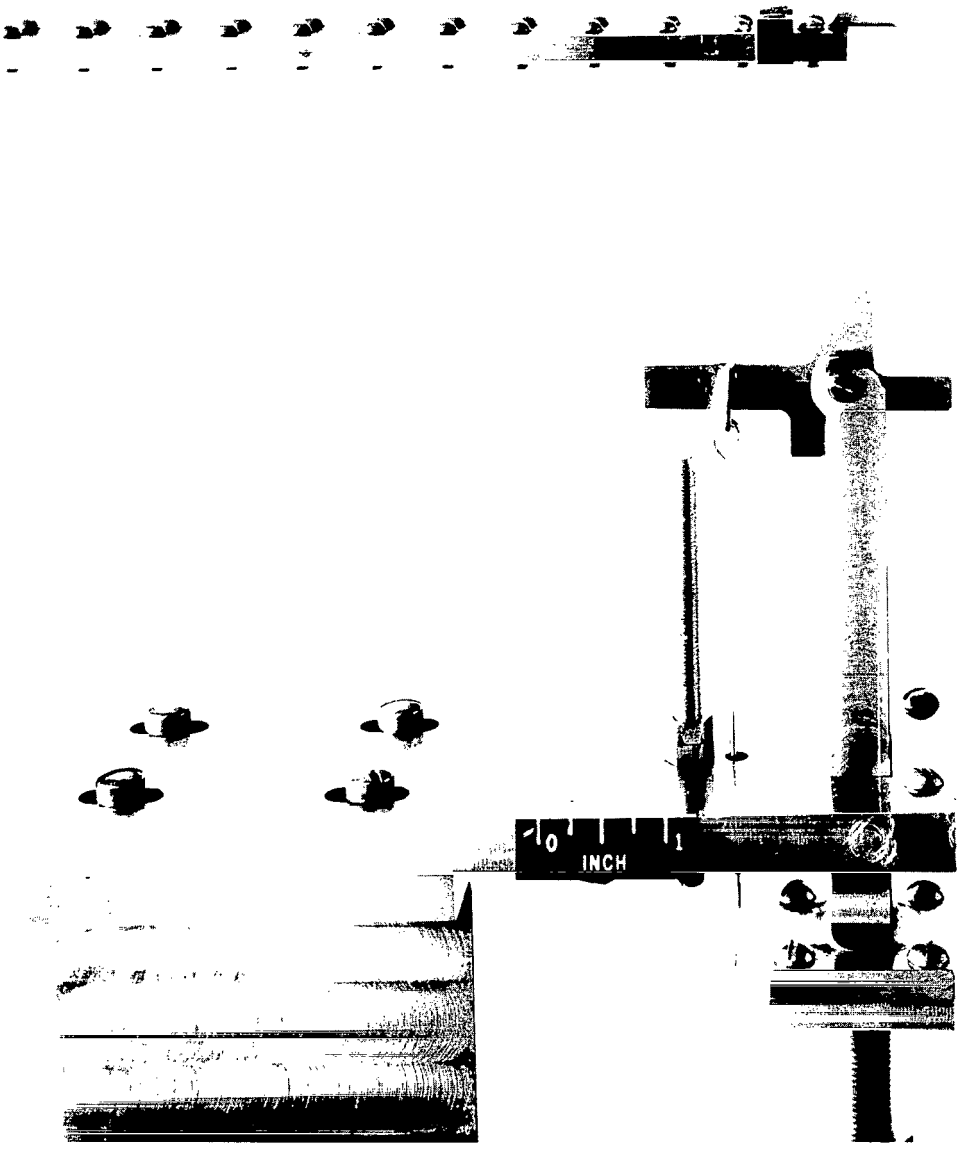

(a) During engagement of beam.

L-63-2000

Figure 8.- Hook-mechanism position.

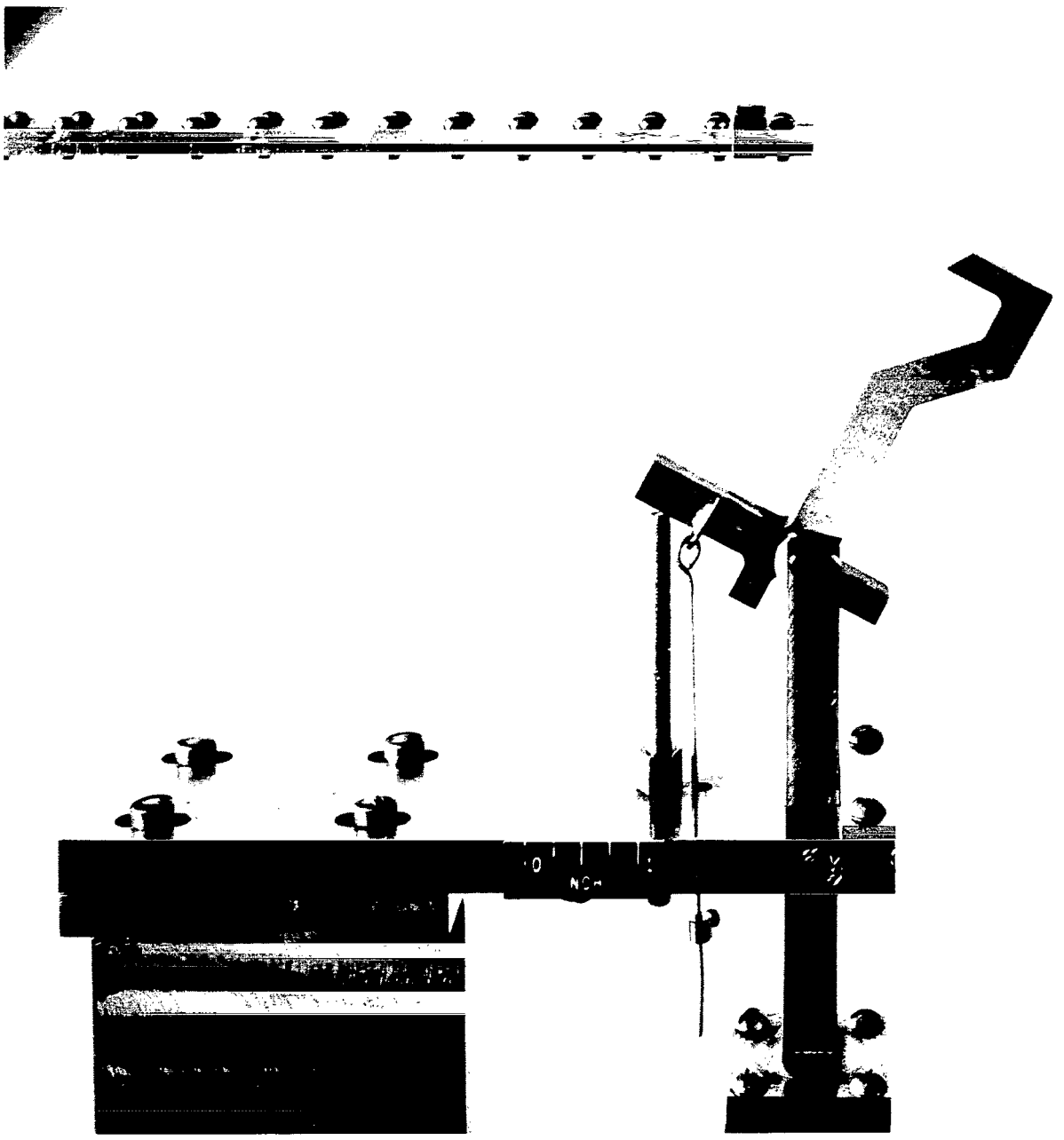

(b) After release of beam. L-63-1996

Figure 8.- Concluded.

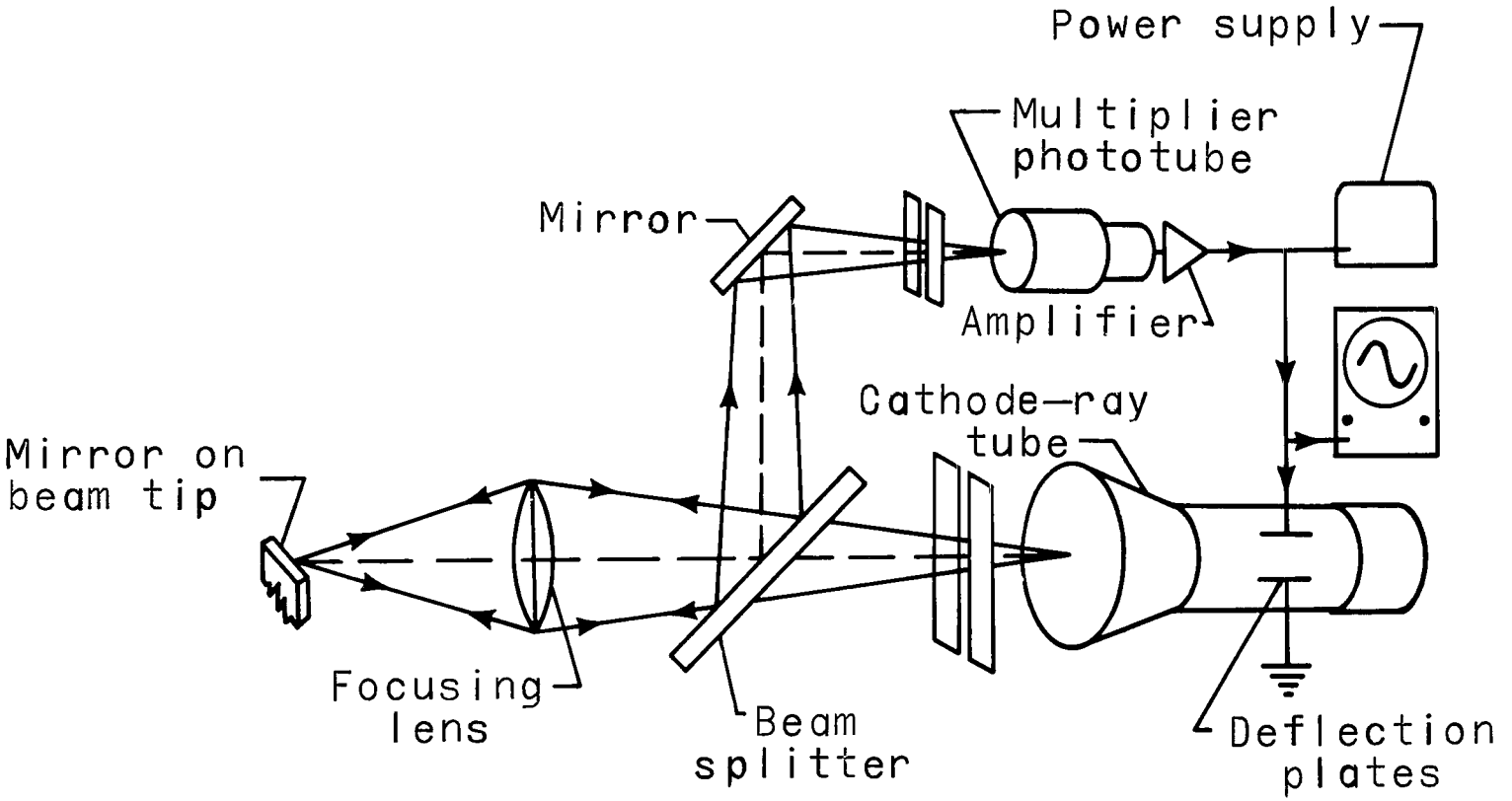

Figure 9.- Schematic diagram of optical-electronic transducer system.

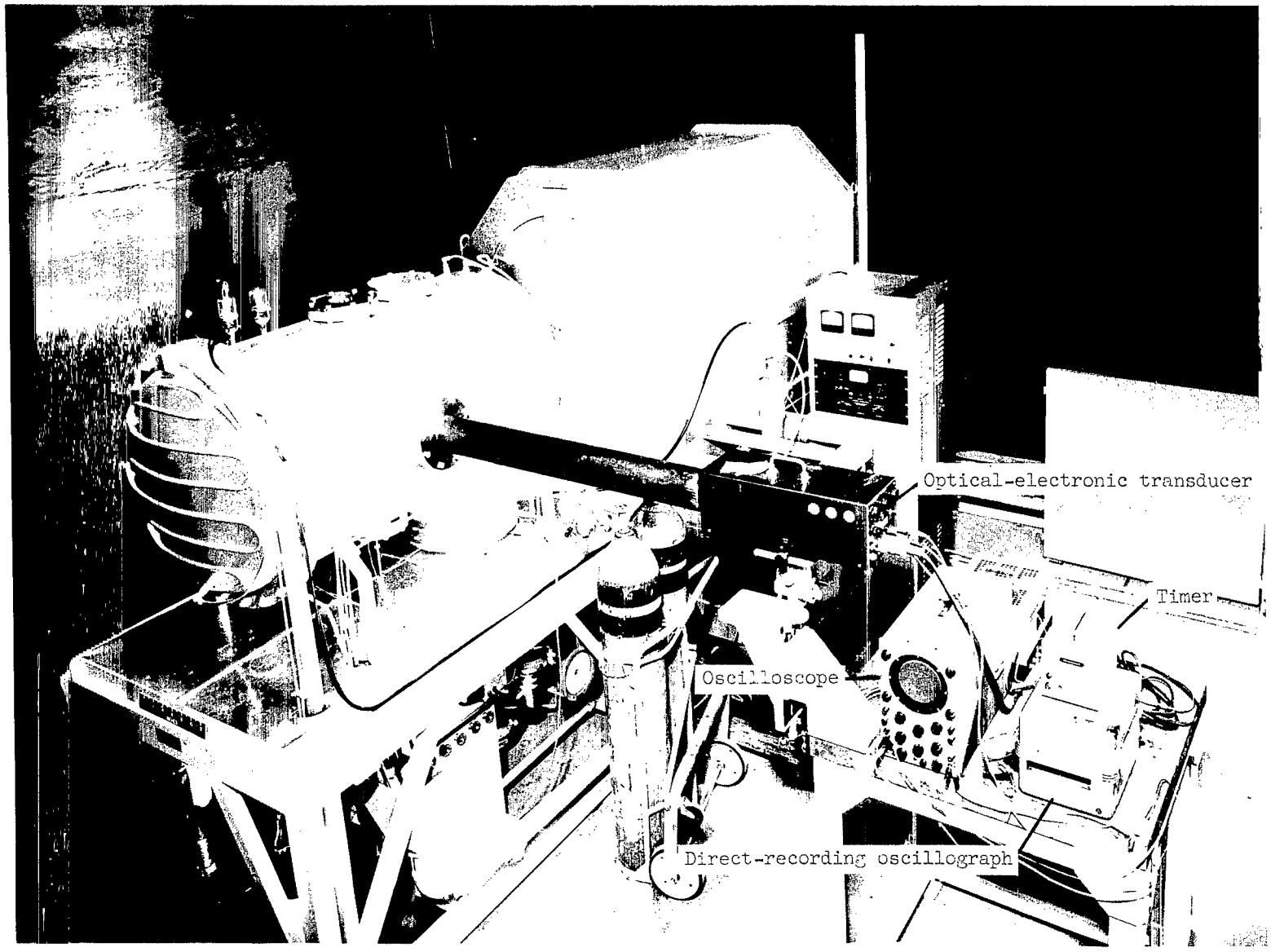

Figure 10.- Test instrumentation for damping measurements.

L-63-1985.1

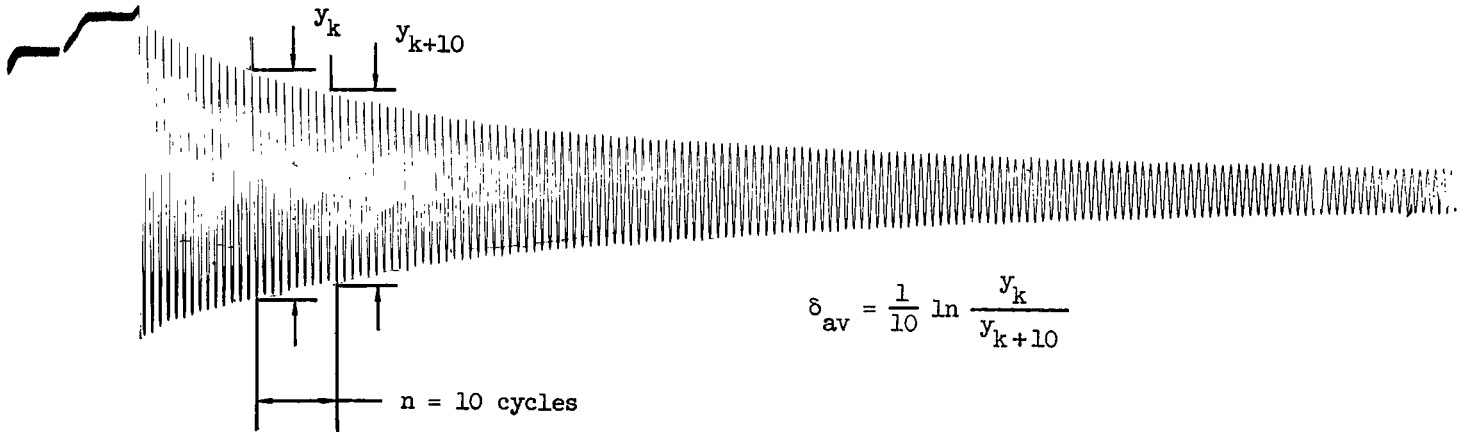

Figure 11.- Typical oscillograph trace of deflection at tip of beam.

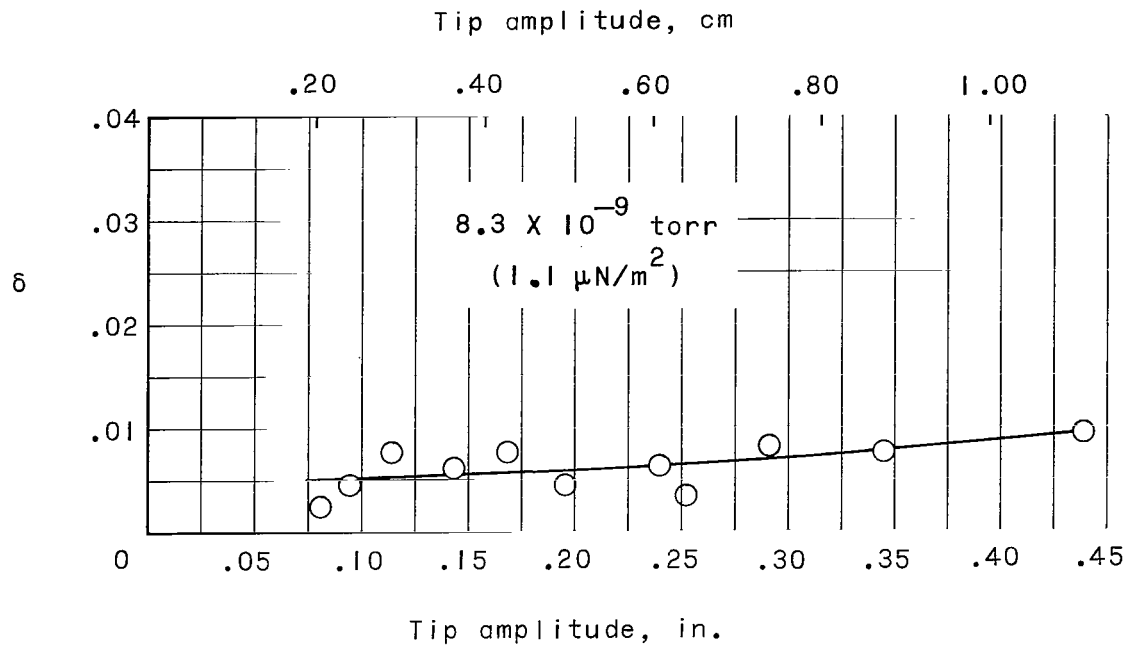

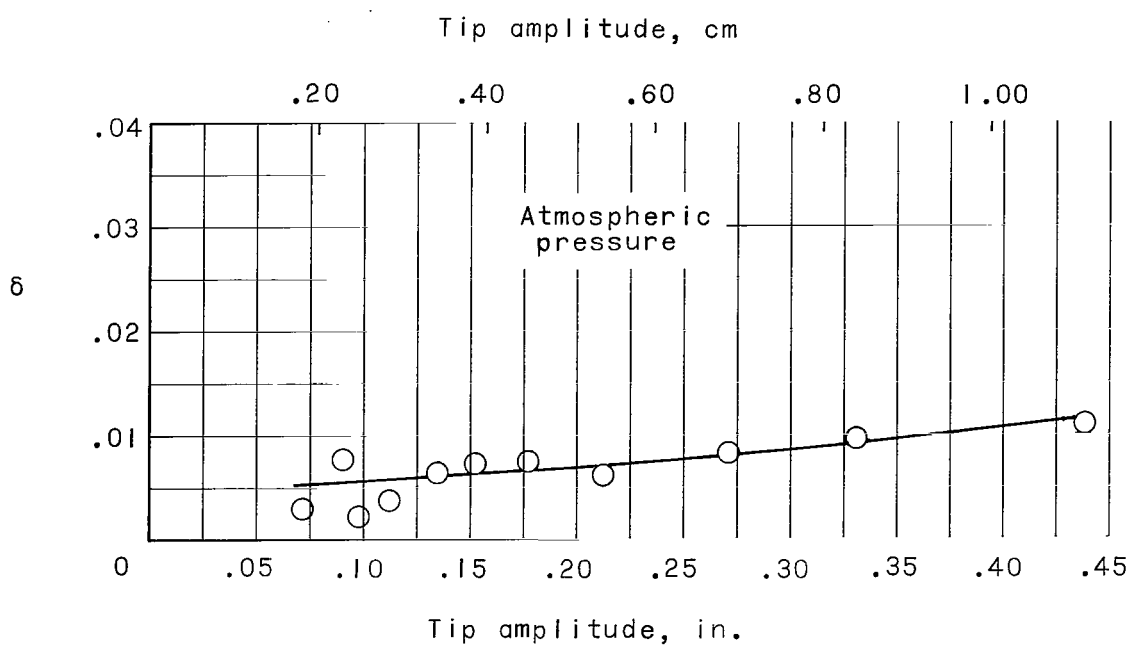

Figure 12.- Variation of logarithmic decrement δ with tip amplitude for solid beam; n = 10 cycles.

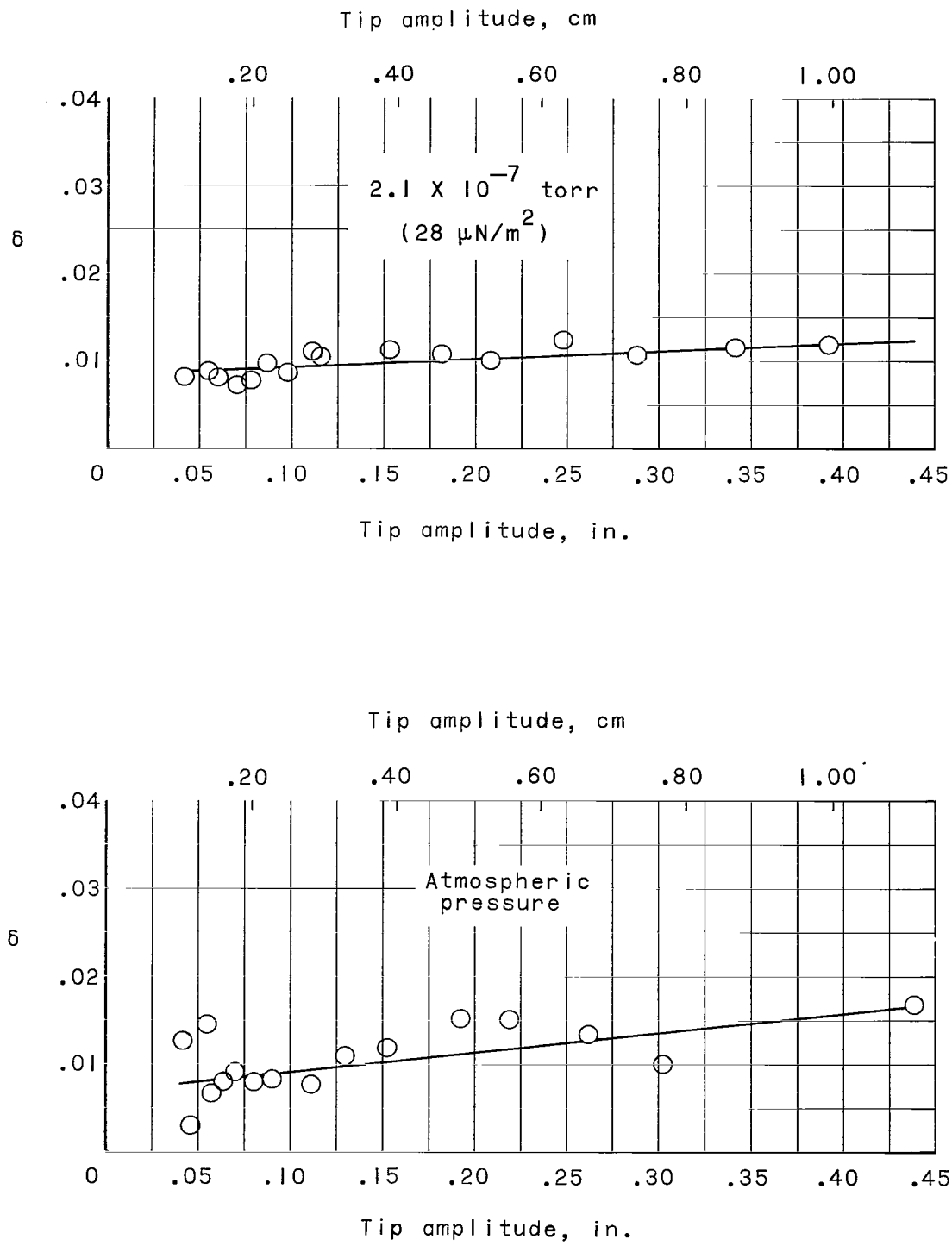

Figure 13.- Variation of logarithmic decrement δ with tip amplitude for rivet-fastened beam; n = 10 cycles.

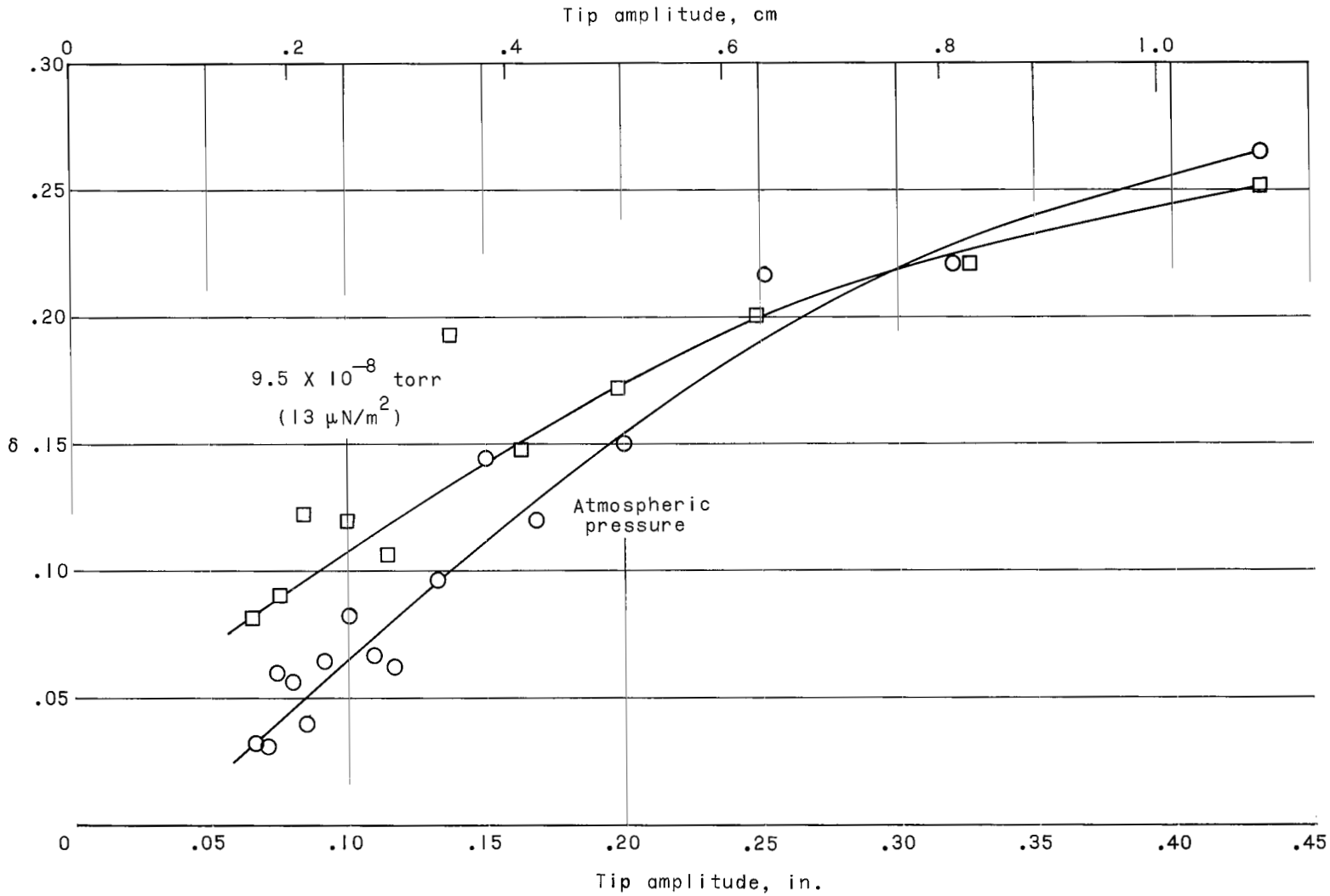

(a) Torque on screws = 0.375 inch-pound (0.0423 m-N); n = 1 cycle.

Figure 14.- Variation of logarithmic decrement δ with tip amplitude for screw-fastened beam.

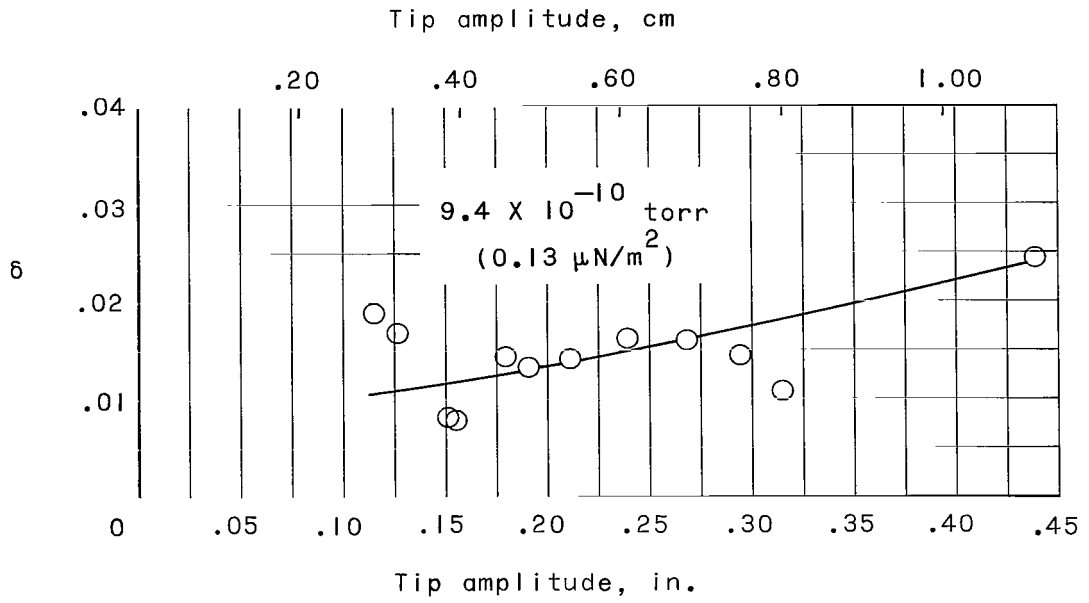

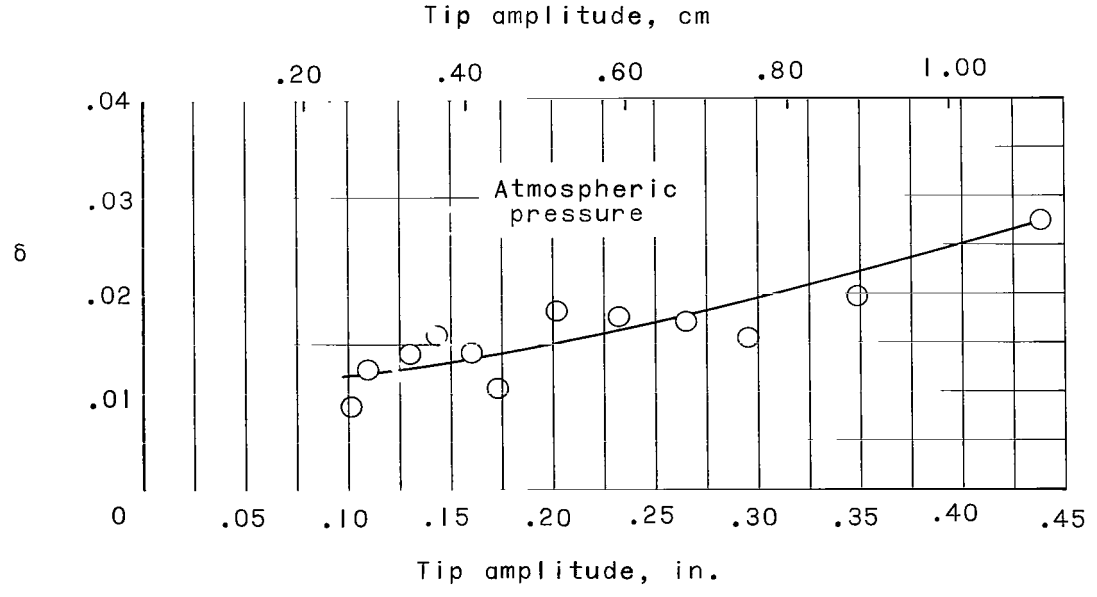

(b) Torque on screws = 5 inch-pounds (0.565 m-N); n = 10 cycles.

Figure 14.- Continued.

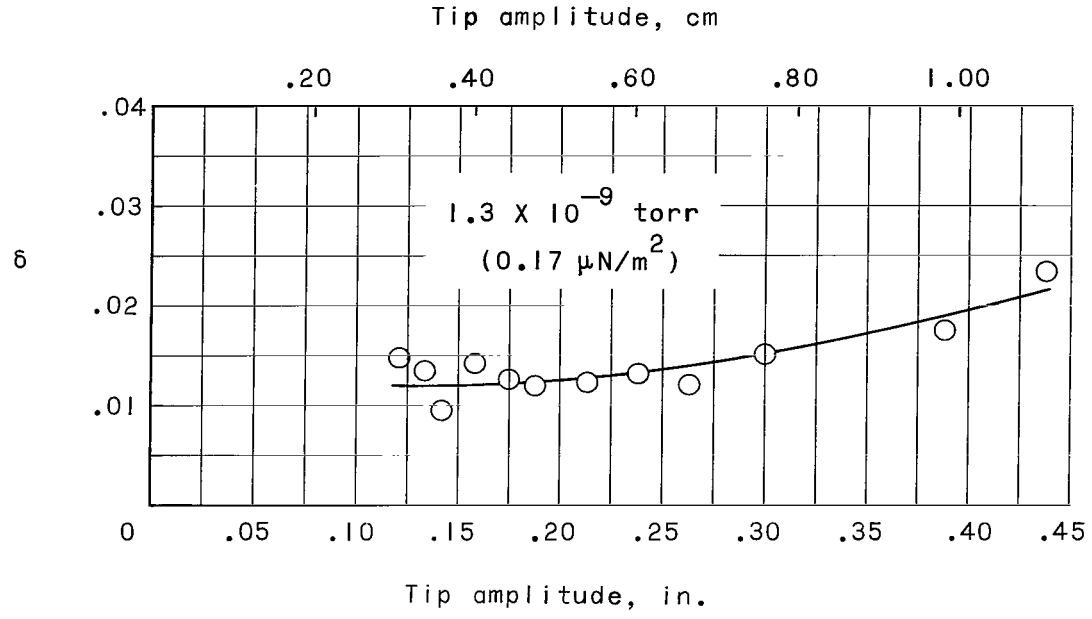

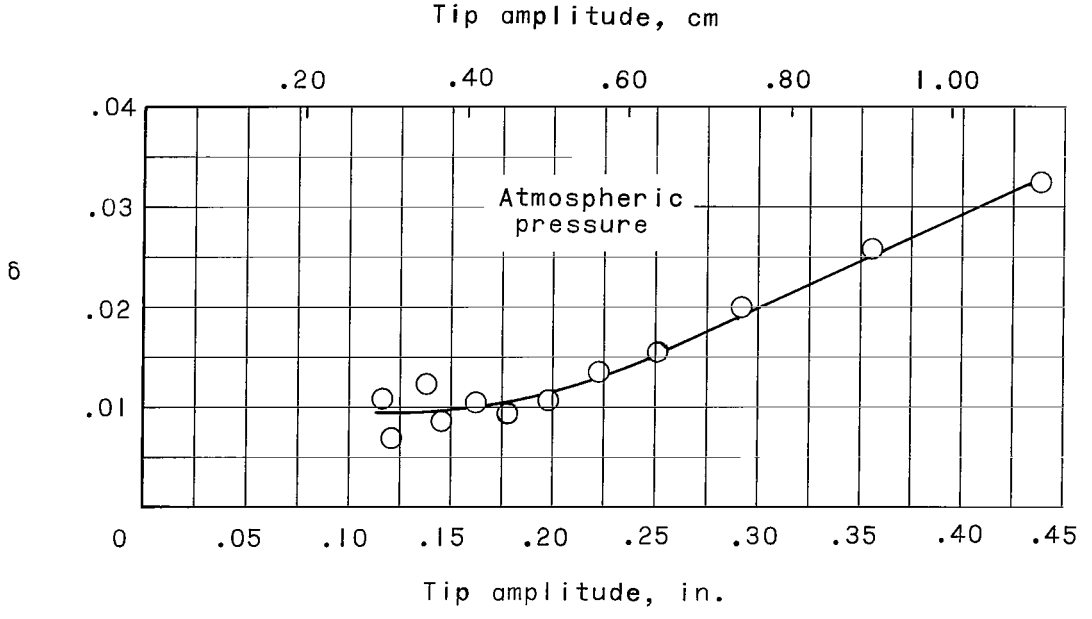

(c) Torque on screws = 10 inch-pounds (1.13 m-N); n = 10 cycles.

Figure 14.- Continued.

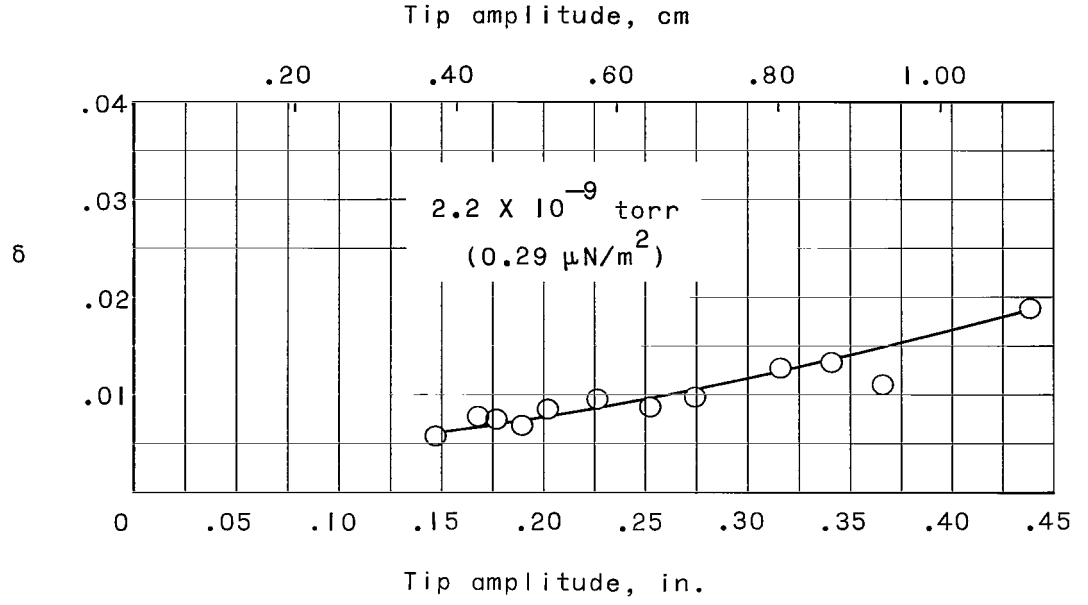

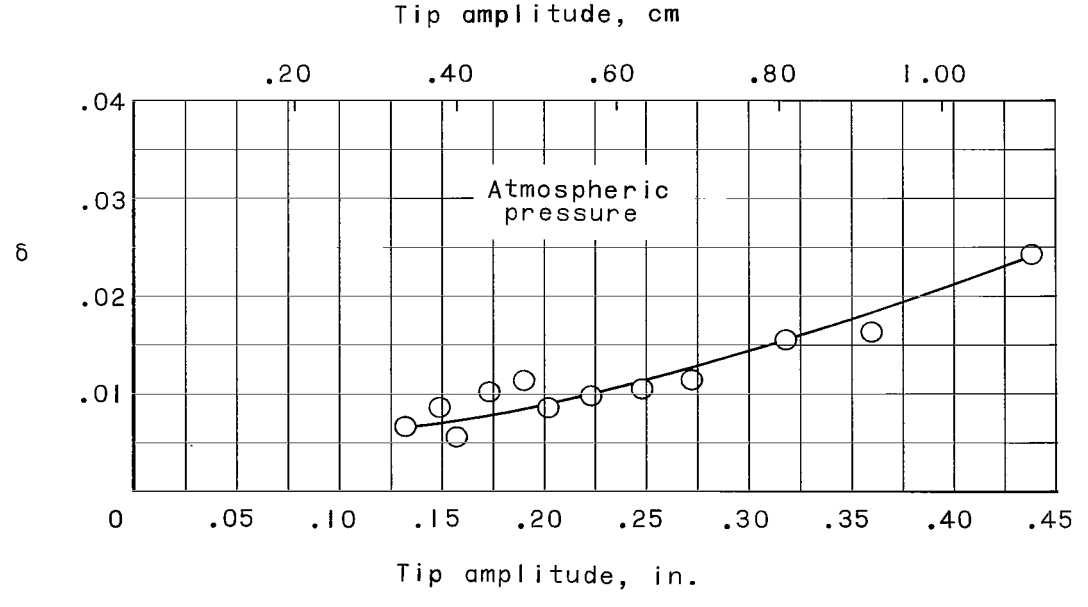

(d) Torque on screws = 15 inch-pounds (1.69 m-N); n = 10 cycles.

Figure 14.- Continued.

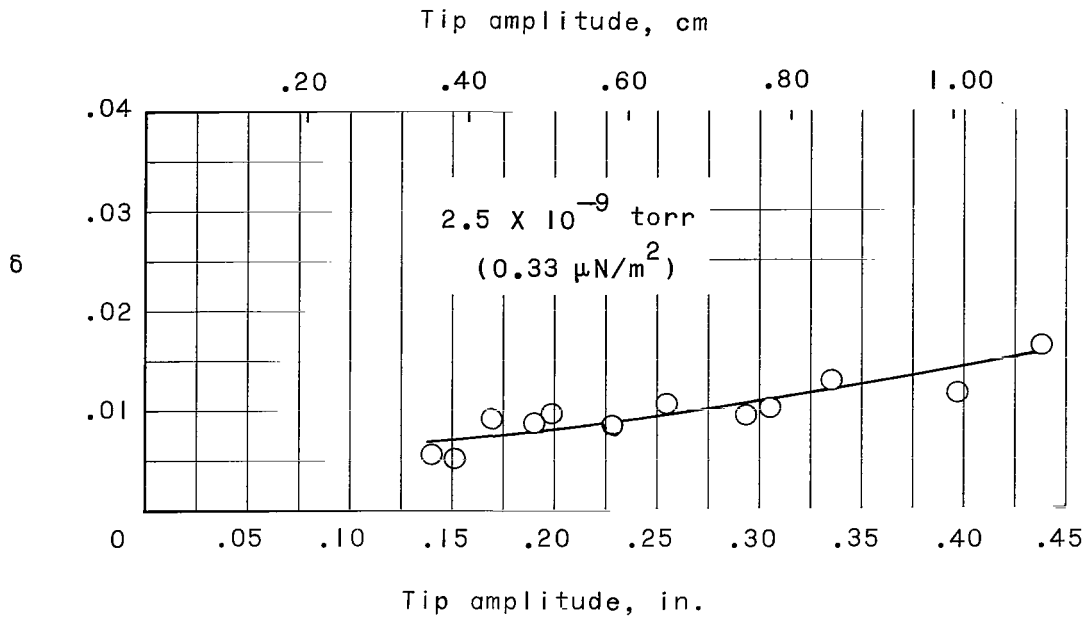

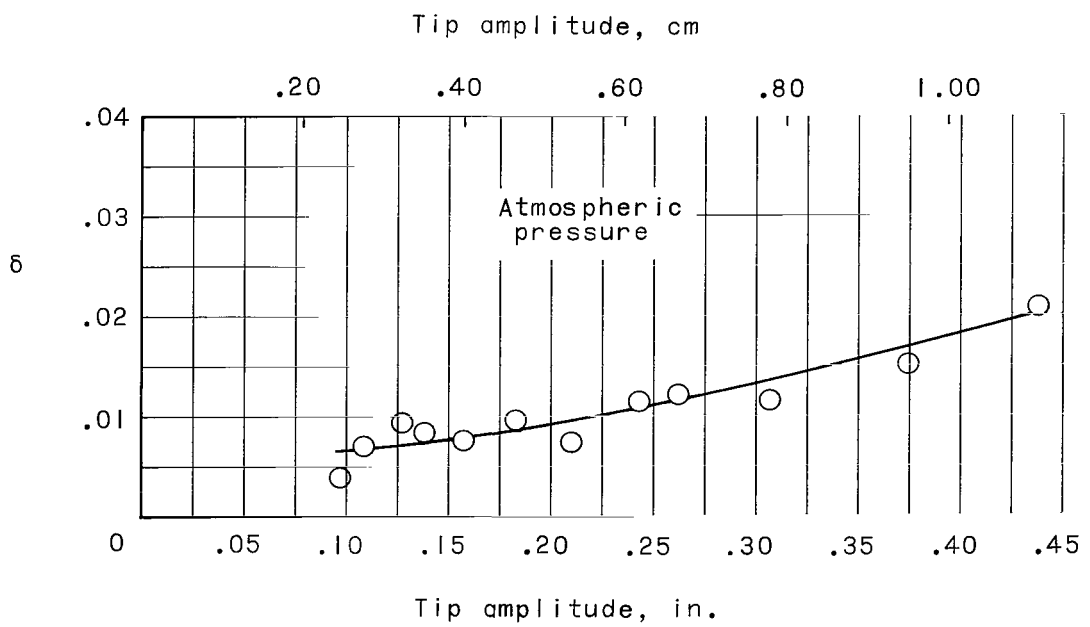

(e) Torque on screws = 20 inch-pounds (2.26 M-N); n = 10 cycles.

Figure 14.- Concluded.

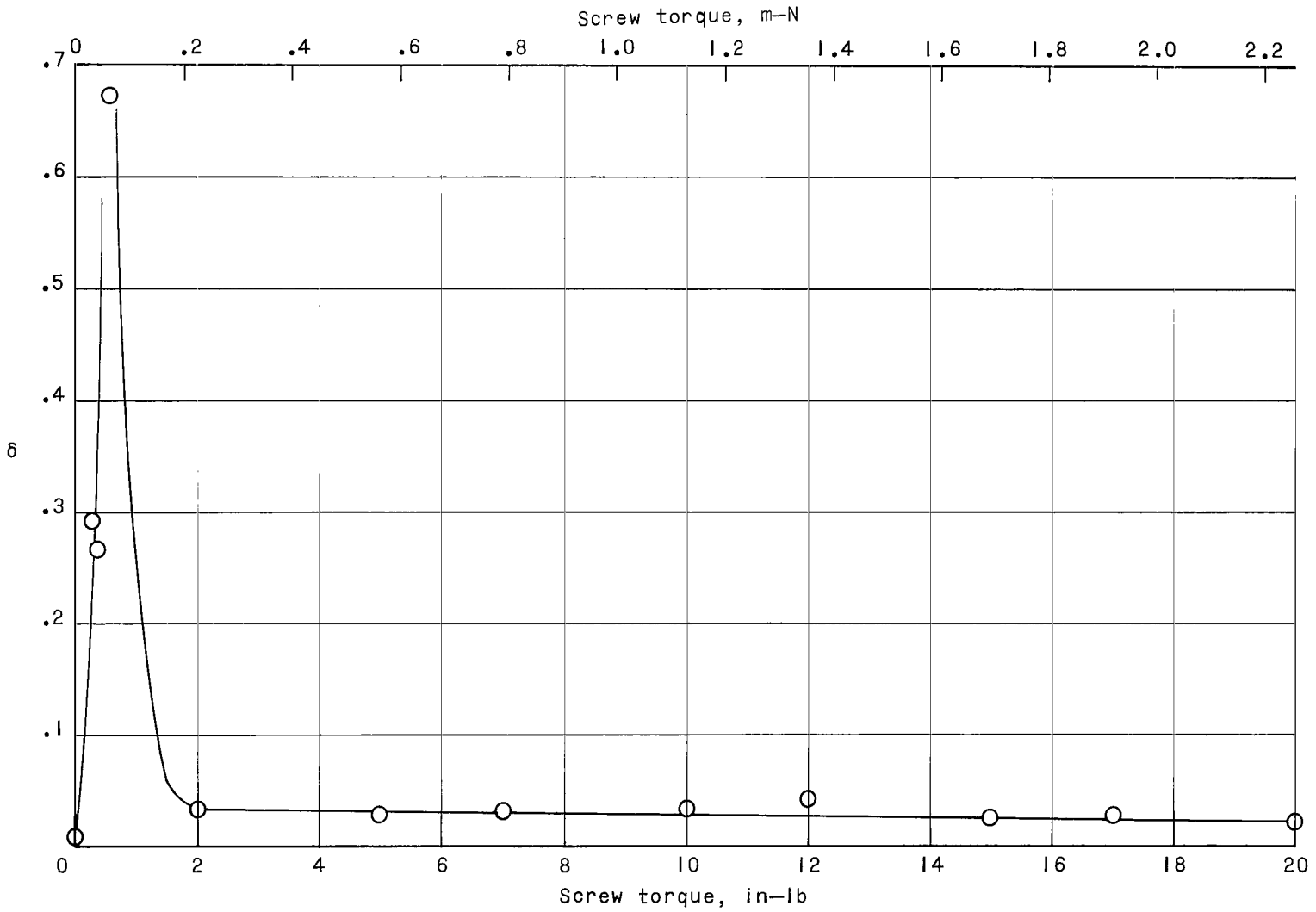

Figure 15.- Variation of logarithmic decrement δ, based on first 10 cycles, with screw torque for tests at atmospheric pressure.

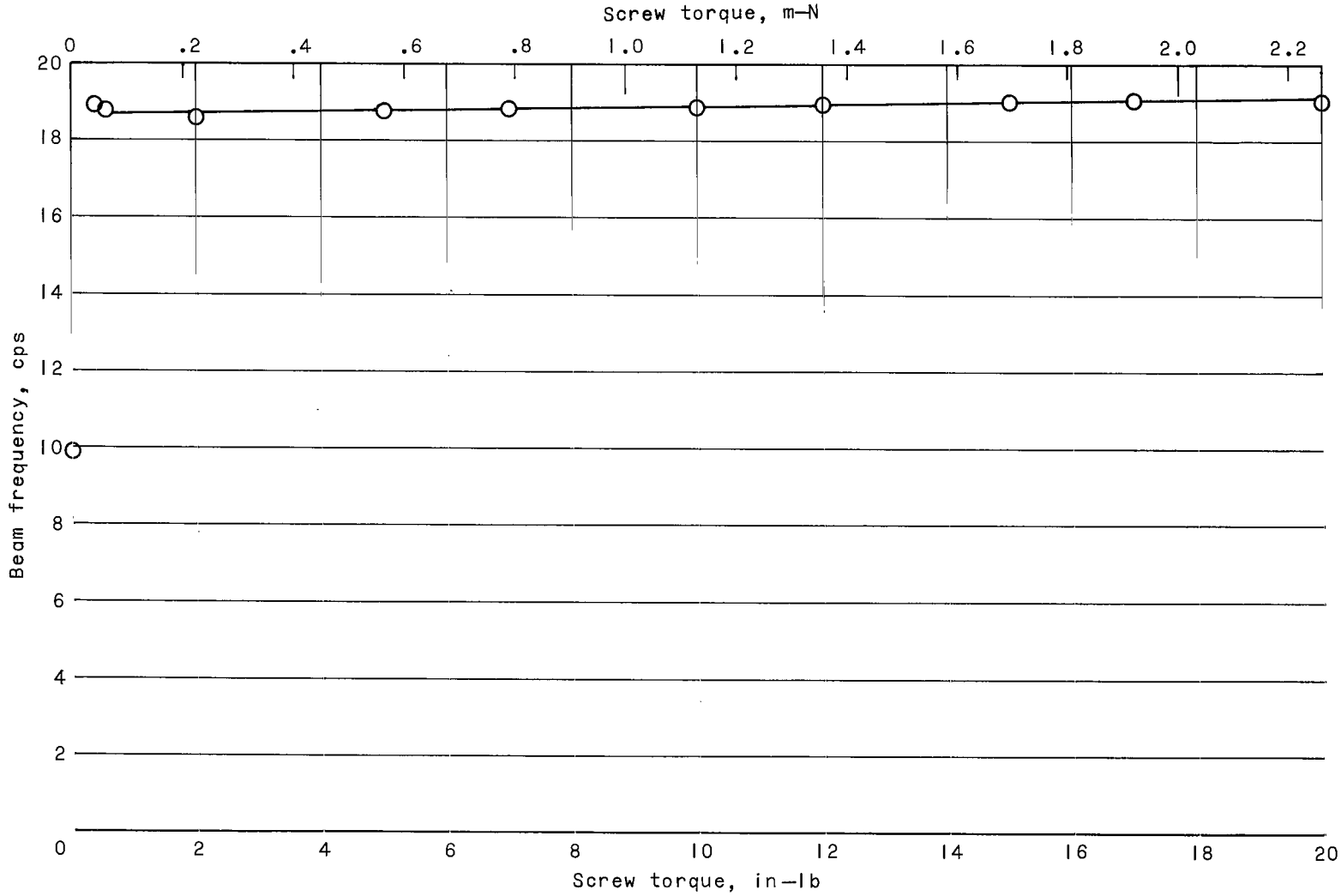

Figure 16.- Variation of beam frequency with screw torque.

3/12/85

"The aeronautical and space activities of the United States shall be conducted so as to contribute . . . to the expansion of human knowledge of phenomena in the atmosphere and space. The Administration shall provide for the widest practicable and appropriate dissemination of information concerning its activities and the results thereof."

—NATIONAL AERONAUTICS AND SPACE ACT OF 1958

NASA SCIENTIFIC AND TECHNICAL PUBLICATIONS

TECHNICAL REPORTS: Scientific and technical information considered important, complete, and a lasting contribution to existing knowledge.

TECHNICAL NOTES: Information less broad in scope but nevertheless of importance as a contribution to existing knowledge.

TECHNICAL MEMORANDUMS: Information receiving limited distribution because of preliminary data, security classification, or other reasons.

CONTRACTOR REPORTS: Technical information generated in connection with a NASA contract or grant and released under NASA auspices.

TECHNICAL TRANSLATIONS: Information published in a foreign language considered to merit NASA distribution in English.

TECHNICAL REPRINTS: Information derived from NASA activities and initially published in the form of journal articles.

SPECIAL PUBLICATIONS: Information derived from or of value to NASA activities but not necessarily reporting the results of individual NASA-programmed scientific efforts. Publications include conference proceedings, monographs, data compilations, handbooks, sourcebooks, and special bibliographies.

Details on the availability of these publications may be obtained from:

SCIENTIFIC AND TECHNICAL INFORMATION DIVISION

NATIONAL AERONAUTICS AND SPACE ADMINISTRATION

Washington, D.C. 20546